Predictions in Ungauged Basins: Promise and Progress (Proceedings of symposium S7 held during the Seventh IAHS Scientific Assembly at Foz do Iguaçu, Brazil, April 2005). IAHS Publ. 303, 2006.

Estimating the potential evapotranspiration over the Yellow River basin by considering the land cover characteristics

M. C. ZHOU, H. ISHIDAIRA & K. TAKEUCHI

Interdisciplinary Graduate School of Medicine and Engineering, University of Yamanashi, Takeda 4-3-11, Kofu 400-8511, Japan

mczhou@ccn.yamanashi.ac.jp

Abstract Hydrological modelling is a powerful tool for decision-makers to manage the large basins effectively. One of the key inputs to hydrological models is the potential evapotranspiration (PET). The Shuttleworth-Wallace (S-W) model is developed for its estimation. In this parameterization, neither experimental measurement nor calibration is introduced. Based on the IGBP land cover classification, the threshold values of vegetation parameters are drawn from the literature. The temporal variation of vegetation LAI is derived from the NOAA-AVHRR NDVI using the SiB2 method. The CRU TS 2.0 database supplies the required meteorological data sets. All these data inputs are publicly available. The developed S-W model is applicable at the global scale, essentially to the data-poor or ungauged large basins. Using the century monthly time series data of CRU TS 2.0 and the monthly composite NOAA-AVHRR NDVI data from 1981 to 2000, annual PET is estimated at 668 mm over the Yellow River basin, much less than the annual reference evapotranspiration (RET) estimated by the FAO-56 method and the pan evaporation (E_{pan}), 968 mm and 1107 mm, respectively. The spatial distribution of PET is markedly non-uniform, from about 345 mm at the source of the river in eastern Tibet with grassland, to about 1168 mm nearby Tongchuan in Shaanxi in the middle stream with deciduous broadleaf forest, and seasonally changes significantly with the LAI.

Key words land cover; NOAA-AVHRR NDVI; physically-based distributed model; potential evapotranspiration; Yellow River

INTRODUCTION

Sustainable management of water resources at the basin scale has become a public awareness and challenges the water authorities. Hydrological modelling is an essential and powerful tool for the decision-makers to manage the large basins effectively. One of the key inputs to the hydrological models is the potential evapotranspiration, which refers to the maximum meteorologically evaporative power on land surface. However, it is difficult to be measured over a large area but usually estimated from the meteorological variables by incorporating the land covers.

A great number of evaporation models have been developed and validated through field measurements, from the single climatic variable driven equations (e.g. Thornthwaite, 1948) to the energy balance and aerodynamic principle combination methods (e.g. Penman, 1948). Among them, probably the Penman equation has the soundest physical basis and is most rigorous. Monteith (1965) generalized the Penman equation, thus called Penman-Monteith method, for water-stressed crops by incorpor-

ating a canopy resistance term. Shuttleworth and Wallace (1985) extended the Penman-Monteith method to sparse vegetation to consider two coupled sources in a resistance network: the transpiration from vegetation and the evaporation from substrate soil. Now the Penman-Monteith (P-M) model and the Shuttleworth-Wallace (S-W) model are widely employed for the estimation of evapotranspiration.

The P-M model treats the vegetation canopy as a single uniform cover, or "big-leaf", but neglects the evaporation from the soil surface. Over a large basin, however, the big leaf assumption is rarely valid. There are often many vegetation types co-existent, and always some parts or periods where or when the vegetation is not "closed". Both the soil surface and the vegetation leaves evaporate or transpire moisture to the atmosphere and their relative importance changes significantly as the vegetation develops. The ideal approach is that applicable at all time and places and able to reflect the effect of changes in surface conditions. The S-W model meets this criterion. Stannard (1993) and Federer *et al.* (1996) compared a number of evapotranspiration models, including the P-M and the S-W, and found that they give very different prediction. The research work of Stannard (1993) and Vorosmarty *et al.* (1998) shows that hydrological modelling is sensitive to PET methods and the S-W model performs best. Therefore the S-W model was selected for this research. The S-W model requires almost the same input data as the P-M model does, but is a highly complex method with many parameters. The parameterization of the S-W model is not straightforward. In this research, only the publicly available data are used. Given they are reliable for the region of interest, this development is applicable at global scale.

METHODOLOGY

The total evapotranspiration in the S-W model is expressed as:

$$\lambda ET = C_c ET_c + C_s ET_s \tag{1}$$

where ET is the evapotranspiration (mm day^{-1}), λ is the latent heat of water vaporization (MJ kg^{-1}), ET_c and ET_s are equivalent to transpiration and evaporation by applying the P-M model to "closed" canopy and bare substrate (MJ m^{-2} day^{-1}), as shown in equations (2) and (3), respectively, C_c and C_s are weighting coefficients as functions of resistances, whose formulation is given by Shuttleworth & Wallace (1985):

$$ET_c = \frac{\Delta(R_n - G) + \left[(24\times 3600)\rho c_p (e_s - e_a) - \Delta r_a^c (R_n^s - G)\right] / (r_a^a + r_a^c)}{\Delta + \gamma\left[1 + r_s^c / (r_a^a + r_a^c)\right]} \tag{2}$$

$$ET_s = \frac{\Delta(R_n - G) + \left[(24\times 3600)\rho c_p (e_s - e_a) - \Delta r_a^s (R_n - R_n^s)\right] / (r_a^a + r_a^s)}{\Delta + \gamma\left[1 + r_s^s / (r_a^a + r_a^c)\right]} \tag{3}$$

where R_n and R_n^s are the net radiation at reference height and substrate soil surface respectively, G is the substrate soil heat flux, all in MJ m^{-2} day^{-1}, e_s and e_a are the saturation and actual vapour pressures respectively (kPa), Δ is the slope of saturation vapour pressure curve (kPa °C^{-1}), ρ is the mean air density (kg m^{-3}), c_p is the specific

heat of moist air (MJ kg^{-1} °C^{-1}), γ is the psychrometric constant (kPa °C^{-1}), r_s^c and r_a^c are the bulk stomatal and boundary layer resistances of canopy, respectively, r_a^s and r_a^a are the aerodynamic resistances between soil and canopy and between canopy and reference height respectively, r_s^s is the surface resistance of soil, all in s m^{-1}.

The parameters of λ, e_s, Δ, ρ, c_p and γ are directly related to air temperature and atmospheric pressure (Shuttleworth, 1993; Allen *et al.*, 1998). The aerodynamic resistances, r_a^s and r_a^a, are obtained by integrating the eddy diffusion coefficients from the soil surface to the "preferred" sink of momentum in canopy and from there to the reference height (K-theory) (Shuttleworth & Gurney, 1990):

$$r_a^s = \frac{h_c \exp(n)}{nK_h}\left[\exp\left(-n z_{0g}/h_c\right) - \exp\left\{-n\left(Z_0 + d_p\right)/h_c\right\}\right] \tag{4}$$

$$r_a^a = \frac{1}{\kappa u_*}\ln\left(\frac{z_a - d_0}{h_c - d_0}\right) + \frac{h_c}{nK_h}\left[\exp\left\{n\left[1 - \left(Z_0 + d_p\right)/h_c\right]\right\} - 1\right] \tag{5}$$

where h_c is the vegetation height (m), n is the eddy diffusivity decay constant of vegetation, set to 2.5 for short vegetation (h_c < 1 m), 4.25 for tall vegetation (h_c > 10 m), and linear interpolation between, K_h is the eddy diffusion coefficient at the top of canopy (m^2 s^{-1}), z_{0g} is the roughness length of ground (m) varying with vegetation type, Z_0 is the "preferred" roughness length (= 0.13h_c) (m), d_p is the "preferred" zero plane displacement (= 0.63h_c) (m), κ is the von Karman's constant (κ = 0.41), u_* is the friction velocity (m s^{-1}), z_a is the reference height (m), set to 2 m above the vegetation. The zero plane displacement and roughness length (m), d_0 and z_0, are estimated as the "preferred" values for a closed canopy (LAI ≥ 4), and using the second-order closure theory for the sparse vegetation. Thus, each term in equations (4) and (5) is given as follows:

$$K_h = \kappa u_*\left(h_c - d_0\right) \tag{6}$$

$$u_* = \kappa u_a / \ln\left\{\left(z_a - d_0\right)/z_0\right\} \tag{7}$$

$$d_0 = \begin{cases} h_c - z_{0c}/0.3 & LAI \geq 4 \\ 1.1h_c \ln\left[1 + \left(c_d LAI\right)^{1/4}\right] & LAI < 4 \end{cases} \tag{8}$$

$$z_0 = \min\left\{0.3\left(h_c - d_0\right),\ z_{0g} + 0.3h_c\left(c_d LAI\right)^{0.5}\right\} \tag{9}$$

where u_a is the wind speed at reference height (m s^{-1}), z_{0c} is the roughness length of "closed" canopy (m), set to 0.13h_c for h_c < 1 m, 0.05h_c for h_c > 10 m, and linear interpolation between, c_d is the mean drag coefficient for individual leaves (Federer *et al.*, 1996) as:

$$c_d = \left[-1 + \exp\left(0.909 - 3.03\, z_{0c}/h_c\right)\right]^4/4 \tag{10}$$

The wind speed at reference height is converted using a logarithmic profile over the weather ground and canopy surface in that the internal boundary layer heights of both surfaces are matched and a step change in surface roughness from z_0 to z_{0w} is assumed:

$$u_a = u_w \frac{\ln(z_b/z_{0w})}{\ln(z_b/z_0)} \frac{\ln[(z_a - d_0)/z_0]}{\ln[(z_w - d_{0w})/z_{0w}]} \tag{11}$$

where u_w is the observed wind speed at height z_w (e.g. 10 m for CRU data (New *et al.*, 1999)), the zero plane displacement (d_{0w}), roughness length (z_{0w}) and the height of internal boundary layer (z_b) at weather station ground are assumed as zero, 0.005 m, and from $z_b = 0.334F_w^{0.875}z_{0w}^{0.125}$ by assuming the fetch F_w = 5000 m, respectively.

The bulk stomatal resistance of canopy is related to environmental variables (Jarvis, 1976):

$$r_s^c = \frac{r_{ST\min}}{LAI_e \prod_i F_i(X_i)} \tag{12}$$

where LAI_e is the effective leaf area index, equal to actual *LAI* for $LAI \le 2$, $LAI/2$ for $LAI \ge 4$ and 2 for between, X_i is any environmental variable, $F_i(X_i)$ is the stress function of X_i, $0 \le F_i(X_i) \le 1$, $r_{ST\cdot\min}$ represents the minimal stomatal resistance of individual leaves under optimal conditions (s m^{-1}). The environmental stress functions, ignoring the concentration of CO_2, are outlined as follows:

$$F_1(S) = (dS)/(c+S) \tag{13}$$

$$F_2(D) = \begin{cases} 1 - 0.409D & \textit{for short vegetation} \\ 1 - 0.238D & \textit{for tall vegetation} \end{cases} \tag{14}$$

$$F_3(T) = \begin{cases} 1 & T \ge 298 \\ 1 - 1.6\times10^{-3}(298 - T)^2 & 273 < T < 298 \\ 0 & T \le 273 \end{cases} \tag{15}$$

$$F_4(\theta) = \begin{cases} 1 & \theta \ge \theta_f \\ \dfrac{\theta - \theta_r}{\theta_f - \theta_r} & \theta_f < \theta < \theta_r \\ 0 & \theta \le \theta_r \end{cases} \tag{16}$$

where S is the incoming photosynthetically active radiation flux (W m^{-2}), $d = 1 + c/1000$, c = 100 for tall vegetation and 400 for short vegetation, D is the air vapour deficit (kPa), $D = e_s - e_a$, T is the air temperature (K), θ, θ_f and θ_r are the actual soil moisture content and these at field capacity and welting point, respectively, in the root zone. For the potential evapotranspiration, $\theta = \theta_f$ is assumed.

The bulk boundary layer resistance of canopy is calculated as:

$$r_a^c = r_b\sigma_b/LAI \tag{17}$$

where σ_b is the shielding factor, taking 0.5, and r_b is the boundary layer resistance of a single leaf as:

$$r_b = \frac{100}{n}\left(\frac{w}{u_h}\right)^{1/2}\left[1-\exp(-n/2)\right]^{-1} \tag{18}$$

where w is the average canopy leaf width (m), u_h the wind speed at top of canopy, from equation (11) by substituting h_c for z_a.

The soil surface resistance, r_s^s, is set to 500 s m^{-1} when the soil moisture in the root zone is at field capacity, following Shuttleworth & Wallace (1985) and Federer *et al.* (1996).

The net radiation over canopy is calculated as the difference between the net solar radiation and longwave radiation. The former can be estimated from the extraterrestrial radiation (function of the Julian date in the year and the latitude location) by considering the cloud cover and the land surface reflectance (or albedo), while the latter from the Stefen-Boltzmann law and corrected with the air humidity and cloud cover. The complete formulation is given by Allen *et al.* (1998). The land surface albedo is expressed as a function of LAI (Uchijima, 1976):

$$\alpha = \alpha_m - (\alpha_m - \alpha_s)\exp(-0.56LAI) \tag{19}$$

where α_m and α_s are the albedo corresponding to the "closed" canopy and the bare soil, respectively. For PET, α_s = 0.1 is used for the wet bare soil and α_m is from the literature and changes with vegetation types.

The radiation reaching the soil surface, R_n^s, is calculated using a Beer's law relationship and the heat conduction into the substrate using the equation of Allen *et al.* (1998): $R_n^s = R_n \exp(-C_r LAI)$ and $G = 0.07(T_{i+1} - T_{i-1})$, respectively, where C_r is the extinction coefficient of the vegetation for net radiation, taking 0.5, T_{i-1} and T_{i+1} are the mean air temperatures in previous and next months (°C), respectively.

Except the soil surface resistance, the parameterization of all resistances and each component of radiation are related to the vegetation parameters such as LAI, height and leaf width. Probably, only the satellite can efficiently provide a frequent measurement to the time-varying vegetation in a long term and over a large area. The value of LAI for each vegetation class is derived from the NOAA-AVHRR NDVI using the SiB2 method (Sellers, 1996):

$$FPAR = FPAR_{\min} + (FPAR_{\max} - FPAR_{\min})\frac{(SR - SR_{\min})}{(SR_{\max} - SR_{\min})} \tag{20}$$

$$LAI = (1 - F_{cl})LAI_{\max}\frac{\ln(1 - FPAR)}{\ln(1 - FPAR_{\max})} + F_{cl}LAI_{\max}\frac{FPAR}{FPAR_{\max}} \tag{21}$$

where SR = (1+NDVI)/(1–*NDVI*), $FPAR$ is the fraction of photo-synthetically active radiation, F_{cl} is the fraction of clumped vegetation, $SR_{\min}$ and $SR_{\max}$ are SR with 5% and 98% of NDVI population. The values of F_{cl}, *NDVI* at 5% and 98% population are adopted from the SiB2. $FPAR_{\min}$ = 0.001 and $FPAR_{\max}$ = 0.950 consider the satellite-sensed NDVI saturation. $LAI_{\max}$ is the maximum LAI when vegetation develops fully.

The vegetation height and leaf width are calculated by differentiating the annual vegetation and perennial vegetation:

$$h_c = h_{c\min} + (h_{c\max} - h_{c\min})\frac{LAI}{LAI_{\max}} \tag{22}$$

$$w = \begin{cases} w_{\max} & \textit{for perennial vegetation} \\ w_{\max}\left[1-\exp\left(-0.6LAI\right)\right] & \textit{for annual vegetation} \end{cases} \tag{23}$$

where $h_{c\max}$ and $h_{c\min}$ are the maximum and minimum vegetation heights (m), and $w_{\max}$ is the maximum leaf width (m). For the perennial vegetation, whose $h_{c\max}$ and $h_{c\min}$ are equal throughout the year.

In the parameterization of the S-W model, a number of threshold parameters for the vegetation canopy and the roughness length for the substrate soil surface are prescribed by referring to the literature according to the IGBP (International Geosphere-Biosphere Programme) land cover classification (Zhou *et al.*, 2006).

DATA SOURCES

In order to apply the S-W model, topographic data, characteristics of land cover and meteorological data are required.

Topographic data

The Hydro1K DEM (digital elevation model) is used to correct the atmospheric pressure, and then the psychrometric constant and air density, γ and ρ. It is a hydrologically proven DEM at 1 km resolution derived by USGS from its 30-second DEM (GTOPO30). The basin part is clipped using the basin boundary, which is manually digitized based on the stream network in the DCW (digital chart of the world). The boundary coverage is also used to clip other basin-spatial data sets in Arc/Info software. The DEM is then averaged into 8 km resolution with 8×8 cells (with the same resolution of downloaded NDVI).

Land cover

The land cover is represented by the IGBP classification at 1 km spatial resolution, as shown in Fig. 1, and is converted into 8 km resolution by assigning the biggest portion of the type among the 8×8 cells to the new cell. In the Yellow River basin, the largest area is the grassland (about 45.6%), second is the croplands or cropland/natural vegetation mosaic (about 25.5%), while the forest area is very small, less than 3.7%, remaining most is shrublands and savannas, taking about 22.5%. The aggregation from 1 km to 8 km makes some small portion land cover types ignored but the general distribution pattern kept.

NDVI data

The monthly NOAA-AVHRR NDVI data are used. It was composite by choosing the highest NDVI from the daily data to avoid the possible effect of cloud cover. The data

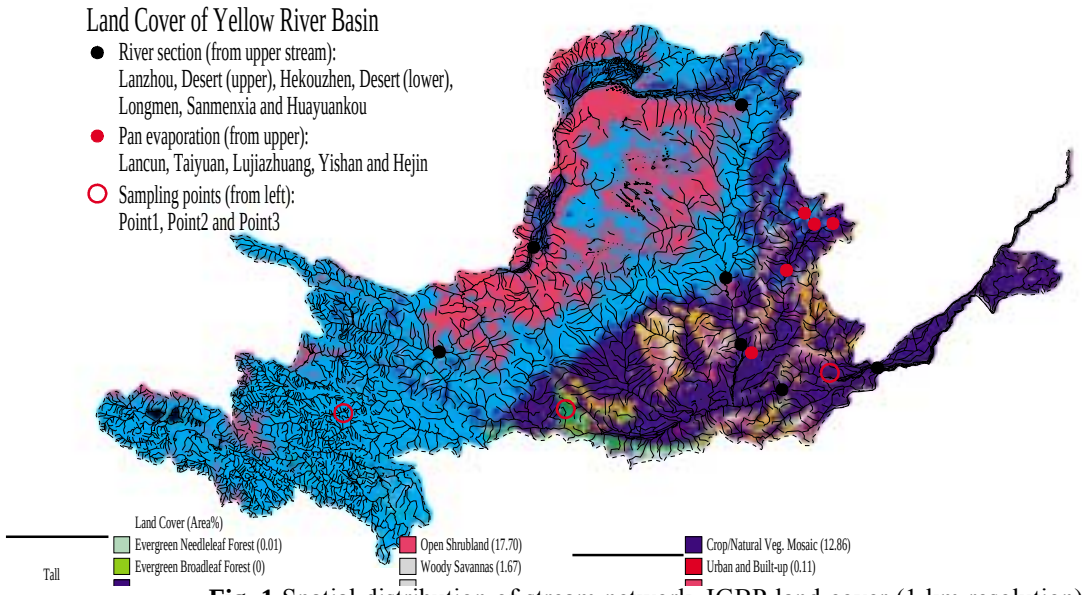

Fig. 1 Spatial distribution of stream network, IGBP land cover (1 km resolution), selected specific points, pan observation sites and critical river sections over Yellow River basin.

is at 8 km resolution covering from 13 July 1981 to 21 September 2001 except the data-missing period from September to December of 1994. The basin part of the NDVI data is clipped using the basin boundary and its Sinusoidal and Mollweide projections, components of the Interrupted Goode Homolosine projection, are transferred into the Lambert Azimuthal Equal Area projection in the Arc/Info software. The monthly NDVI data are assumed to represent the mid-day of the month. The average monthly NDVI data from 1981 to 2000 are used before 1981 and the data-missing period.

Meteorological data

The required meteorological data include temperature, humidity, radiation and wind speed. The CRU (Climate Research Unit, University of East Anglia in UK) TS 2.0 provided the monthly time series data of the daily mean temperature, diurnal temperature range, cloud cover and actual vapour pressure from 1901 to 2000 and mean monthly wind speed averaged in 1961–1990 for the global at 0.5 × 0.5° grids (New *et al.*, 1999, 2000). The wind speed was measured at a majority of 10 m height (New *et al.*, 1999). In construction of CRU TS 2.0, climatic variables are separated into two categories: primary and secondary. Regarding the data used in this study, the primary variables include daily mean temperature and diurnal temperature range and were constructed directly from station observations. The secondary variables include cloud cover and vapour pressure and were constructed by merging the station observations where available with the synthetic data derived from the gridded primary variables. For the synthetic data, the cloud cover was related to the diurnal temperature range using an empirical equation and the actual vapour pressure to the daily minimum

temperature using a conceptual equation (New *et al.*, 2000). The CRU data sets are extracted at the Yellow River basin and transferred into the Lambert Azimuthal Equal Area projection at 8 km resolution without interpolation involvement. All climatic variables change significantly in the year and are distributed very non-uniformly over the basin.

RESULTS

By the S-W method, annual PET is estimated as 610–724 mm with an average of 668 mm from 1901 to 2000 over the whole basin, the minimum occurring in 1964 and the maximum in 1997. Comparing the inter-annually change, its spatial distribution is much more non-uniform because of the very different climate types and the heterogeneity of vegetation cover over the basin. Figure 2 shows the yearly change of annual PET over the whole basin and at three arbitrarily chosen points: grassland in Tibet, forest in middle stream and cropland in lower stream, as shown in Fig. 1. Although the yearly changes are almost coincident over the basin, at the three points, their magnitudes and variation amplitudes are quite different. Among the three points, PET is lowest and yearly change gentle at Point 1 (grassland in Tibet) (from 479 to 610 mm with an average of 555 mm) due to its cold weather and short vegetation; highest and yearly change significantly at Point 2 (cropland in the lower stream) (from 828 to 1074 mm with an average of 974 mm) although the vegetation is shorter and the location is almost at the same latitude but has quite different climate type from at Point 3 (forest in the middle stream) (from 712 to 988 mm with an average of 830 mm). Figure 3 shows the basin-spatial distribution of annual PET averaged in 1901–2000. The least is located at the source of the river in the eastern Tibet with the grassland (34°21′52.9″N and 96°28′22.7″E), only about 345 mm year^{-1}, while the largest is nearby Tongchuan in Shaanxi in the middle stream with the deciduous broadleaf forest (35°27′29.5″N and 109°58′45.7″E), about 1168 mm year^{-1}. The area with PET larger than 1168 mm year^{-1} shown in Fig. 3 corresponds to the water surface.

As a directly standardized P-M method, the FAO-56 is popularly used to estimate RET for a hypothetical crop that closely resembles an extensive green grass surface

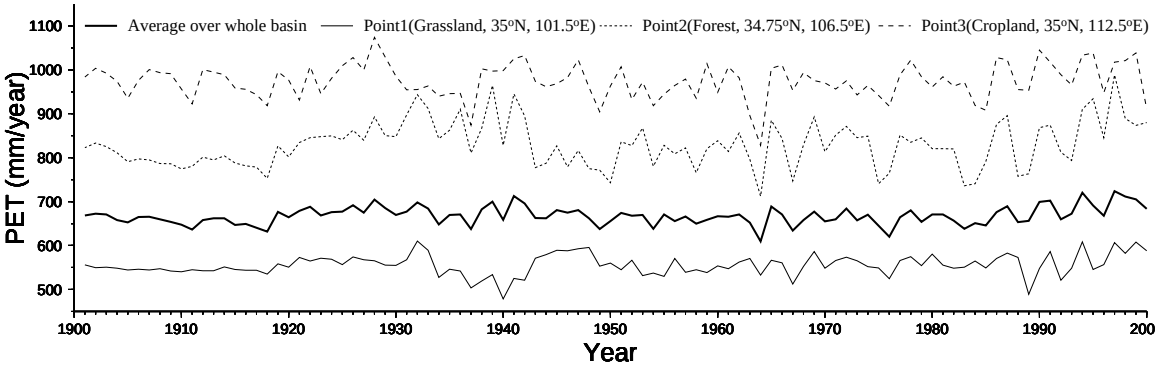

Fig. 2 Yearly change of annual PET over the whole basin and at three points: Point 1 in eastern Tibet in upper stream, Point 2 in middle stream and Point 3 in lower stream.

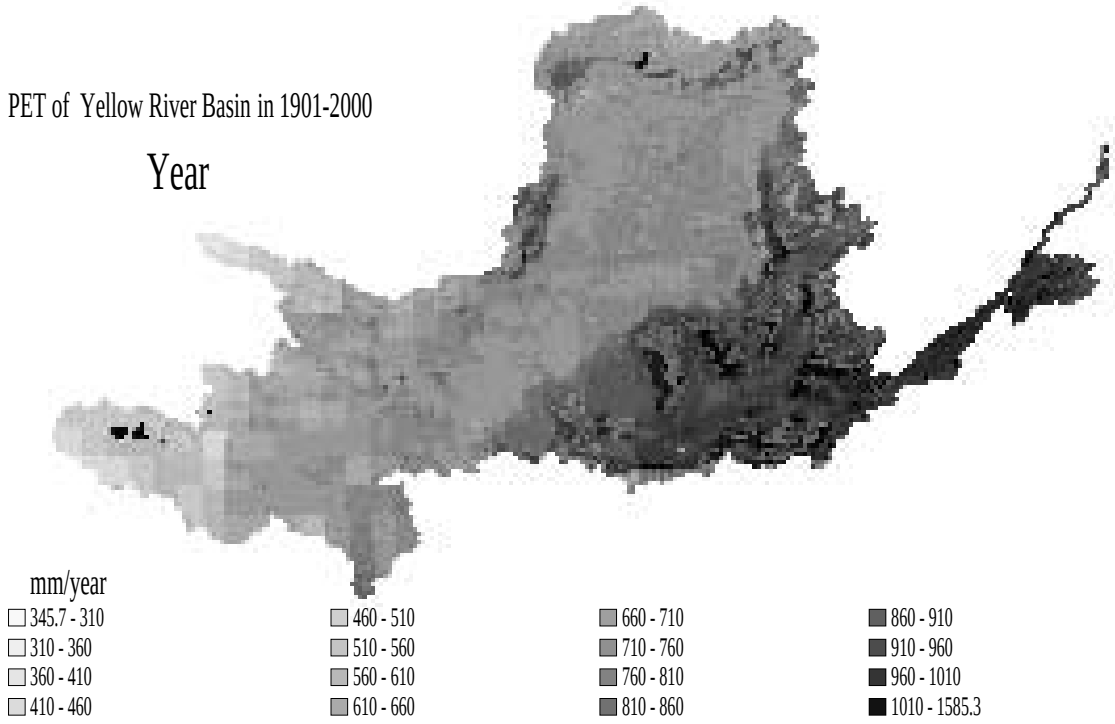

Fig. 3 Spatial distribution of annual PET averaged in 1901–2000.

with uniform height (0.12 m), actively growing (canopy resistance of 70 s m^{-1}), completely shading the ground (albedo of 0.23) and with adequate water (Allen *et al.*, 1998):

$$RET = RET_1 + RET_2 \tag{24}$$

$$RET_1 = \frac{\Delta}{\Delta + \gamma} 0.408(R_n - G) \tag{24a}$$

$$RET_2 = \frac{\gamma}{\Delta + \gamma} \frac{u_2}{(1 + 0.34u_2)} \frac{900}{(273 + T)} (e_s - e_a) \tag{24b}$$

where all notations have the meanings and are calculated the same as in the S-W model except u_2 represents the wind speed at 2 m height (m s^{-1}) and is converted from other height using $u_2 = 4.87u_w / \ln(67.8z_w - 5.42)$. Because the FAO-56 does not use spatial distribution of vegetation types and their development stages, the RET can be considered as an integrated climatic index.

The pan evaporation (E_{pan}) is referenced at five sites of the Fenhe tributary between 35°30′N~38°00′N and 110°30′E~113°00′E within a square of 2.5° both in latitude and in longitude in Shanxi Province (Ibbitt *et al.*, 2002) and for the upper basins above some sections along the main river (Chen, 1996), as shown in Fig. 1. The pan type is ϕ20 for the sites except unknown at Taiyuan, and the observation period is from 1971 to 1990. For the upper basins, the pan observation is from the 601 (a standard pan in China), and the period was not reported thus assumed representing the whole century.

The annual PET, RET and E_{pan} are compared in Table 1 for these specific sites and upper basins. At the five sites, estimated RET is almost at the same level although

located at different latitude. Actually from south to north, the daily mean temperature, actual vapour pressure, cloud cover and net radiation all decrease in turn from Hejin, Yishang, Lujiazhuang and Lancun except some climatic variables are a bit higher only at Taiyuan, which may be in a city. The wind speed does not change much among these sites. As a result, their radiation component, RET_1, decreases and the saturation humidity deficit component, RET_2, increases from south to north except is different a bit at Taiyuan. Both RET_1 and RET_2 are consistent with their geographical locations. The combined effect of radiation and saturation humidity deficit makes RET almost at the same level in the long term. It is possible in this particular region. Actually, their annual RET is different in each year, with a maximum difference of about 50 mm year^{-1}, and changes from year to year. The change figure of annual RET is not shown here. The pan evaporation, however, is quite different among these sites, and most are higher than RET, i.e. at Taiyuan, Lujiazhuang and Yishang, but less at Lancun or similar to at Hejin. This is because RET is an areal climatic estimate while the point observation of E_{pan} is seriously affected by local micro-climate, the instrument type and its operation and maintenance. On the other hand, the PET is also not in the same

Table 1 Comparison of annual potential evapotranspiration (PET), reference evapotranspiration (RET) and pan evaporation (E_{pan}) (mm year^{-1}).

Pan (latitude, longitude and altitude) or sub-basin (location and area)	IGBP land cover (Area%)	PET	RET	E_{pan}
Lancun (38°00′N, 112°26′E and 880 m)	Cropland	770	1015	986
Taiyuan (37°46′N, 112°37′E)	Grassland	635	1028	1719
Lujiazhuang (37°44′N, 113°03′E and 900 m)	Cropland	717	1020	1395
Yishang (37°00′N, 111°50′E and 760 m)	Cropland/natural vegetation mosaic	810	1015	1157
Hejin (35°34'N, 110°48'E and 379 m)	Cropland	856	1015	1008
Tibetan plateau (226 944 km^2 in upper basin)	Grasslands (92%)	550	886	800
Lanzhou-Hekouzhen (188 416 km^2 in middle basin)	Open shrublands (48%) Grasslands (41%)	622	1011	1470
Hekouzhen-Longman (126 976 km^2 in middle basin)	Grasslands (47%), Open shrublands (29%), Cropland/natural vegetation mosaic (17%)	668	1029	1200
Longman-Sanmenxia (194 304 km^2 in middle basin)	Cropland/natural vegetation mosaic (36%), Croplands (21%), Grasslands (21%)	773	949	1050
Sanmenxia-Huayuankou (41 664 km^2 in middle basin)	Croplands (41%), Cropland/natural vegetation mosaic (23%), Deciduous broadleaf forests (16%), Closed shrublands (14%)	883	1033	1060
Huayuankou-Outlet (26 880 km^2 in lower basin)	Croplands (89%)	914	1126	1200
Desert pass on Mongolia plateau (110 912 km^2 in middle basin)	Open shrublands (60%), Grasslands (38%)	613	1040	1700
Whole basin (805 184 km^2)	Grasslands (48%), Open shrublands (18%), Cropland/natural vegetation mosaic (13%), Croplands (12%)	668	968	1107

level among these sites. However, the PET reflects not only the vegetation types but also the vegetation development states, of course, furthermore the areal climatic pattern. For example, s m^{-1} in the S-W model (Zhou *et al.*, 2006), degenerates the evaporation significantly. To apply RET or E_{pan} as input to hydrological models, crop and/or pan coefficients must be multiplied and they are often subjectively determined. But the PET avoids this conversion and can be directly input.

CONCLUSIONS

This study developed the S-W model for estimating the long-term PET over large basins using the parameter values from the literature and publicly available database. Its application to the Yellow River basin shows that the PET is not only controlled by the climate patterns, but also changes with the vegetation types and their development. The CRU TS 2.0 meteorological database, IGBP land cover classification, and particularly the satellite NDVI which measures the dynamic change of vegetation morphology with environmental conditions (e.g. the prolonged water stress) and seasons, provide the S-W model with complete data sets over a large basin in a long term. Given these public data are reliable for the interesting region, this development is applicable at the global scale, essentially to the data-poor or ungauged large basins. The estimated PET can be input directly to a hydrological model without any conversion by multiplying factors as for the use of RET or E_{pan}.

Acknowledgements We are pleased to acknowledge the financial support of the Core Research for Evolutional Science and Technology (CREST) Program of Japan Science and Technology Corporation (JST) through the research project of "Sustainable Watershed Management in the Yellow River".

REFERENCES

Allen, R. G., Pereira, L. S., Raes, D. & Smith, M. (1998) Crop evapotranspiration—guidelines for computing crop water requirements. FAO Irrigation and Drainage Paper, no. 56. FAO, Rome, Italy.

Chen D. X. (ed.) (1996) *Hydrology of Yellow River*. Yellow River Water Resources Press, Zhengzhou, China. (in Chinese).

Federer, C. A., Vorosmarty, C. J. & Fekete, B. (1996) Intercomparison of methods for potential evapotranspiration in regional or global water balance models. *Water Resour. Res.* **32**, 2315–2321.

Ibbitt, R., Takara, K., Desa, M. N. M. & Pawitan, H. (ed.) (2002) *Catalogue of Rivers for Southeast Asia and the Pacific*, Volume IV. UNESCO-IHP Regional Steering Committee.

Jarvis, P. G. (1976) The interpretation of the variation in leaf water potential and stomatal conductance found in canopies in field. *Phil. Trans. Roy. Soc. London*, **B273**, 593–610.

Monteith, J. L. (1965) Evaporation and environment. In*: Symp. Soc. Exp. Bio. XIX*, 205–234. Cambridge University Press, Cambridge, UK.

New, M., Hulme, M. & Jones, P. (1999) Representing twentieth-century space-time climate variability. Part I: Development of a 1961–90 mean monthly terrestrial climatology. *J. Climate* **12**, 829–856.

New, M., Hulme, M. & Jones, P. (2000) Representing twentieth-century space-time climate variability. Part II: Development of 1901–96 monthly grids of terrestrial surface climate. *J. Climate* **13**, 2217–2238.

Penman, H. L. (1948) Natural evaporation from open water, bare soil and grass. *Proc. Roy. Soc. London* **A193**, 120–146.

Sellers, P. J., Los, S. O., Tucker, C. J., Justice, C. O., Dazlich, D. A., Collatz, G. J. & Randall, D A. (1996) A revised land surface parameterization (SiB2) for atmospheric GCMs. Part II: the generation of global fields of terrestrial biophysical parameters from satellite data. *J. Climate* **9**, 706–737.

Shuttleworth, W. J. & Gurney, R. J. (1990) The theoretical relationship between foliage temperature and canopy resistance in sparse crops. *Quart. J. Roy. Met. Soc*. **116**, 497–519.

Shuttleworth, W. J. & Wallace, J. S. (1985) Evaporation from sparse crops—an energy combination theory. *Quart. J. Roy. Met. Soc.* **111**, 839–855.

Shuttleworth, W. J. (1993) Evaporation. In: *Handbook of Hydrology* (ed. by D. R. Maidment), 4.1–4.53. McGraw-Hill, New York, USA.

Stannard, D. I. (1993) Comparison of Penman-Monteith, Shuttleworth-Wallace, and modified Priestley-Taylor evapotranspiration models for wildland vegetation in semiarid rangeland. *Water Resour. Res*. **29**(5), 1379–1392.

Thornthwaite, C. W. (1948) An approach toward a rational classification of climate. *Geograph. Rev.* **38**, 55–94.

Uchijima, Z. (1976) Maize and rice. In: *Vegetation and the Atmosphere* (ed. by J. L. Monteith), 33–64. Academic Press, London, UK.

Vorosmarty, C. J., Federer, C. A. & Schloss, A. L. (1998) Potential evaporation functions compared on US watersheds: possible implications for global-scale water balance and terrestrial ecosystem modelling. *J. Hydrol*. **207**, 147–169.

Zhou, M. C., Ishidaira, H., Hapuarachchi, H. P., Magome, J., Kiem, A. S. & Takeuchi, K. (2006) Estimating potential evapotranspiration using the Shuttleworth-Wallace model and NOAA-AVHRR NDVI to feed a distributed hydrological model over the Mekong River basin. *J. Hydrol*. DOI: 10.1016/j.jhydrol.2005.11.013 (in press).